



Empirical fragility curves of engineered steel and RC residential buildings after Mw 7.3 2017 Sarpol-e-zahab earthquake

Mahnoosh Biglari¹ · Antonio Formisano² · Behrokh Hosseini Hashemi³

Received: 11 November 2020 / Accepted: 29 March 2021 / Published online: 5 April 2021
© The Author(s), under exclusive licence to Springer Nature B.V. 2021

Abstract

This study investigates the damage data after November 12, 2017, Iran earthquake (M_w 7.3), collected on 440 steel and reinforced concrete residential buildings. Structures have low-to-medium height and are located in Sarpol-e-zahab city, as well as in the west and northwest parts of Kermanshah province, Iran. The peak ground acceleration demands are determined according to data of the micro-shakemap of Sarpol-e-zahab city and the shakemap of Kermanshah province, while the mean values of intensities are determined from the existing empirical relationship between PGA and intensity. The investigated buildings are engineered steel and RC structures nominally erected according to the second and third editions of the Iranian code for earthquake-resistant buildings, but mostly under careless supervision and with low-quality materials. Damage probability matrix, vulnerability index and empirical fragility curves are presented for three subgroups of steel and RC structures on the basis of (i) structural materials and seismic resistant systems (i.e. braced, moment and combination of braced and moment steel frames, as well as moment and combination of moment and shear wall RC frames), without considering the height of structures; (ii) structural materials and height of structures, without considering the seismic resistant systems (i.e. low and medium-height steel and RC structures); (iii) structural materials, without considering the seismic resistant systems and height of structures (i.e. total data for steel and RC frames). The proposed fragility curves are compared with other fragility curves for steel and RC buildings from previous studies. Finally, since this earthquake was the first seismic event in Iran affecting a considerable number of steel and RC engineered buildings, the proposed empirical fragility curves are definitely unique and crucial for realistic damage and vulnerability assessment of similar buildings in future earthquake scenarios, as well as for developing rapid seismic loss assessment after damaging earthquakes.

Keywords Sarpol-e-zahab earthquake · Fragility curves · Steel and RC buildings · Iranian building typology · Seismic vulnerability assessment

✉ Mahnoosh Biglari
m.biglari@razi.ac.ir; mahnooshbiglari@yahoo.com

Extended author information available on the last page of the article

1 Introduction

Recent destructive earthquakes in Iran are highlighting the seismic vulnerability of steel and reinforced concrete (RC) buildings. These structures were nominally constructed under the Iranian seismic design code, but they were mostly built under careless construction supervision and with low-quality materials, that have brought up damages and ended in significant casualties and injuries, as well as financial losses. This has emboldened the need for the development of realistic fragility curves for different seismic resisting building types.

It is almost 30 years that engineered steel and RC residential buildings are constructed in Iran. Data from the 2018 census in Iran revealed that from 1986 to 2016 the number of steel and RC structures increased from 2.9 to 57% of the total number of buildings. The number of masonry buildings erected in this period shows that the majority of the new constructions are engineered steel and RC buildings. Meanwhile, many cities in Kermanshah province, like Sarpol-e-zahab, at the western and southwestern outskirts of Iran bordering Iraq, were rebuilt after the devastation of the Iran-Iraq war in the late 1980s, leading to new buildings mainly made of steel, RC and confined masonry structures. Sarpol-e-zahab was at a distance of about 35 km from the epicenter of M_w 7.3 2017 earthquake, which was the first earthquake in Iran that largely affected engineered and masonry structures. This earthquake provided unique information about the performance of various types of Iranian steel and RC structures. Biglari and Formisano (2020) presented DPMs, vulnerability indices and empirical fragility curves from damage data based on the RISK-UE level 1 method (LM1, Risk-UE 2004), on both unreinforced masonry (URM) and confined masonry (CM) buildings after both M_w 7.3, 2017 Sarpol-e-zahab earthquake and M_w 6.6, 2003 Bam earthquake of Iran.

In this paper, the damage database of engineered residential steel and RC buildings after M_w 7.3 2017 earthquake is analyzed to propose the empirical fragility curves. The earthquake triggered the greatest damage on Sarpol-e-zahab city, as well as on the west and northwest parts of Kermanshah province. To propose the fragility curves in terms of PGA, the seismic site response analyses in Sarpol-e-zahab city (Ashayeri et al. 2021), along with the recorded PGA at Iranian Strong Motion Network (ISMN), and the shakemap of the earthquake for Kermanshah province (Firuzy et al. 2018), have provided the expected PGA that was experienced by each investigated structure during the earthquake. In this way, the uncertainty of the expected strong-motion beneath each investigated building was tackled, which is commonly noticed as the shortcoming of empirical fragility curves. The collected data are categorized into three groups in terms of seismic resistant systems and the height of structures. Then, each damage data is correlated to PGA and EMS-98 intensity (Grünthal 1998) demand based on the buildings' locations. Finally, DPMs, vulnerability indices, and corresponding empirical fragility curves for building classes are presented and compared with previous fragility curves of Iranian steel and RC buildings, as well as with empirical fragility curves of Italian RC buildings.

2 Seismic input data

On 2017 November 12th an earthquake of magnitude M_w 7.3 hit the Kermanshah province, killing at least 620 people. Ezgeleh, with a population of 1500 inhabitants, was the city closest to the epicenter (10 km northwest). Tazeabad city, with about 15,000 inhabitants and 35 km east of the epicenter, and Sarpol-e-zahab city, with about 56,000 inhabitants and placed 35 km south of the epicenter, were seriously damaged. The event was attributed to a known fault zone named Mountain Front Fault (MFF) that extends almost north to south along the Iran–Iraq border with the strike direction of the north-west to the south-east (Tatar et al., 2018).

Comprehensive ambient noise analyses in the form of array measurements and single-station measurements for seismic microzonation of Sarpol-e-zahab city were performed after this earthquake by Ashayeri et al. (2020). Subsequently, Ashayeri et al. (2021) performed the seismic site response analysis and presented the ground motion shakemap of Sarpol-e-zahab city due to M_w 7.3 earthquake, also providing the Peak Ground Accelerations (PGAs) on the location of the buildings at Sarpol-e-zahab city. Furthermore, for the other earthquake shock-affected regions, PGAs were extracted from accelerograms of Iran Strong Motion Network (ISMN, provided by Road, Housing, & Urban Development Research Center) at KRK (Kerend city), ELA (Eslamabad city), MHD (Mahidasht city), KRM1&2 (Kermanshah city), JAV (Javanroud city), RVN (Ravansar city), GRS (Gor-e-sefid) and SUM (Sumar city) stations, along with GMPEs-derived shakemap by Firuzi et al. (2018).

The mean values of intensity are determined from the relationship between PGA and macroseismic intensity (Eq. 1), which was proposed by Gomez-Capera et al. (2020):

$$\text{LogPGA} = -1.446 + 4.134\text{Log}I_{MCS} \quad (1)$$

where PGA is expressed in cm/s^2 and I is expressed according to Mercalli–Cancani–Sieberg scale (Sieberg 1930). This novel PGA-IMCS relationship does not saturate in high values of intensity, but, by assuming a 1 to 1 relationship between MCS and European Macroseismic Scale (EMS-98) (Grünthal 1998) intensities (Azzaro et al. 2004) for intensities higher than VI, it is found as the most suitable equation in the literature.

3 Damage grades and building typology

The damage ratio parameter is defined as the ratio between the repairing cost and the reconstruction one of the building. In this study, the EMS-98 (Grünthal 1998) is used for estimating the damage grade that is defined as apparent damage to be determined in the emergency following an earthquake disaster. According to this scale, the RC building damages are classified into six grades as follows:

Grade 0 (D0): No damage.

- Grade 1 (D1): Negligible to slight damages (no structural damage, slight non-structural damage). Fine cracks in plaster over frame members or in walls at the base. Fine cracks in partitions and infills.
- Grade 2 (D2): Moderate damage (slight structural damage, moderate non-structural damage). Cracks in columns and beams of frames and structural walls. Cracks in



Fig. 1 Examples of damage grades to steel and RC structures during 2017 Sarpol-e-zahab earthquake

Table 1 The building typology matrix

Main type	Description	Height	No. of stories	No. of investigated buildings
Steel (S)	Braced frame (X)	Low-rise (L)	1–3	18
		Mid-rise (M)	4–6	20
	Moment resisting frame (M_0)	Low-rise (L)	1–3	50
		Mid-rise (M)	4–6	7
	Combination of moment resisting frame and braced frame (C)	Low-rise (L)	1–3	97
Reinforced Concrete (RC)	Moment resisting frame (M_0)	Mid-rise (M)	4–6	30
		Low-rise (L)	1–3	57
	Combination of moment resisting frame and RC shear wall (C)	Mid-rise (M)	4–6	32
		Low-rise (L)	1–3	4
		Mid-rise (M)	4–6	25

partition and infill walls; fall of brittle cladding and plaster. Falling mortar from the joints of wall panels.

- Grade 3 (D3): Substantial to heavy damage (moderate structural damage, heavy non-structural damage). Cracks in columns and beam-column joints of frames at the base and joints of coupled walls. Spilling of concrete cover, buckling of reinforced rods. Large cracks in partition and infill walls, failure of individual infill panels.
- Grade 4 (D4): Very heavy damage (heavy structural damage, very heavy non-structural damage). Large cracks in structural elements with compression failure of concrete and fracture of rebars; bond failure of beam reinforced bars; tilting of columns. The collapse of either few columns or a single upper floor.
- Grade 5 (D5): Destruction (very heavy structural damage). The collapse of the ground floor or parts (e.g. wings) of buildings.

The steel buildings' damage grades are assumed similar to RC buildings' ones. Figure 1 shows examples of damage grades to steel and RC structures during the 2017 Sarpol-e-zahab earthquake.

The earthquake damage data were gathered at the rapid assessment level from Kalantari et al. (2019). The field house to house inspection was carried out after the Sarpol-e-zahab earthquake. It provided a database on ordinary masonry, steel and RC buildings. Table 1 presents the building typology matrix of the collected and mapped structural damage data. Engineered structures of the earthquake-affected area may be divided into 10 subgroups based on basic structural material, system and building height. The investigated structural systems for steel buildings (S) can be divided into three seismic resistant systems: braced frames (X), moment resisting frames (Mo) and a combination of both moment-resisting frames and braced frames (C). As for RC buildings, they are divided into two systems: moment resisting frames (Mo) and a combination of moment-resisting frames and RC shear walls (C). Each system can be categorized into two different height levels: low-rise structures (L), with 1–3 stories, and mid-rise structures (M), with 4–6 stories. Thus, each structure with a specific system and height is briefly defined by a combination of these capital letters, which will henceforth be displayed in graphs and tables.

Steel braced frames refer to the structures where the frames, made of beams and columns connected to each other with pinned joints, are designed for vertical loads, while concentric/eccentric braces carry and transfer all horizontal loads (e.g. earthquake and wind) to the foundation. Steel and RC moment resisting frames are made of beams and columns having full-rigid joints which are designed for bearing both horizontal and vertical loads. The combined structural behavior, leading to the so-called dual constructions, refer to structures in which the braced frames are used for one load direction and moment frames are used for the other direction. The main issues of the Iranian steel and RC structures are the low quality of welding and the low quality of concrete, respectively.

In Table 1, the number of statistical data collected for each category is shown. Since the number of surveyed buildings in some of these categories (SXL, SXM, SMoM, RCCL, and RCCM) is not sufficient (less than 30) to provide the trustworthy damage probability matrixes (DPMs), vulnerability indices (V_1 s) and fragility curves, the categories are subsequently combined for two types of steel and RC structures. Table 2 shows the final combined structural typology matrix. It is categorized in three groups: (1) based on structural materials and seismic resistant systems without considering the height of the structures; (2) based on structural materials and heights of the structures without considering the seismic resistant systems; (3) based on structural materials without considering the seismic resistant systems and height of structures. Finally, the results of the damage probability matrix, vulnerability index and fragility curves in terms of PGA and intensity are presented for these three groups. Among all groups, only RCC (RC structure with a combination of moment resisting frame and RC shear wall) has less than 30 data, so that DPM and V_1 are provided, but fragility curves are not derived.

Figure 2 shows the cumulative percentage of each damage grade for all three groups of investigated structures. The most recurrent damage grade for the first group is D2, with 52% of occurrence for RC buildings with a combination of moment resisting frame and RC shear wall. In the second group, the most repeated damage grade is D4 for low-rise RC structures (36% of occurrence). Finally, for the third group, the most repeated damage grade is D4 for RC structures (25% of occurrence).

Table 2 The combined structural typology matrix

Group	Type	Structural description	Data combination	No. of Investigated Buildings
1	SX	Steel braced frame	SXL + SXM	38
	SM ₀	Steel moment frame	SM ₀ L + SM ₀ M	57
	SC	Combination of moment resisting frame and braced frame	SCL + SCM	127
	RCM ₀	reinforced concrete moment frame	RCM ₀ L + RCM ₀ M	89
	RCC	Combination of moment resisting frame and RC shear wall	RCCL + RCCM	29
2	SL	Low-rise steel	SXL + SM ₀ L + SCL	165
	SM	High-rise steel	SXM + SM ₀ M + SCM	57
	RCL	Low-rise reinforced concrete	RCM ₀ L + RCCL	61
	RCM	High-rise reinforced concrete	RCM ₀ M + RCCM	57
3	SAII	Steel	SXL + SM ₀ L + SCL + SXM + SM ₀ M + SCM	222
	RCAII	Reinforced concrete	RCM ₀ L + RCCL + RCM ₀ M + RCCM	118

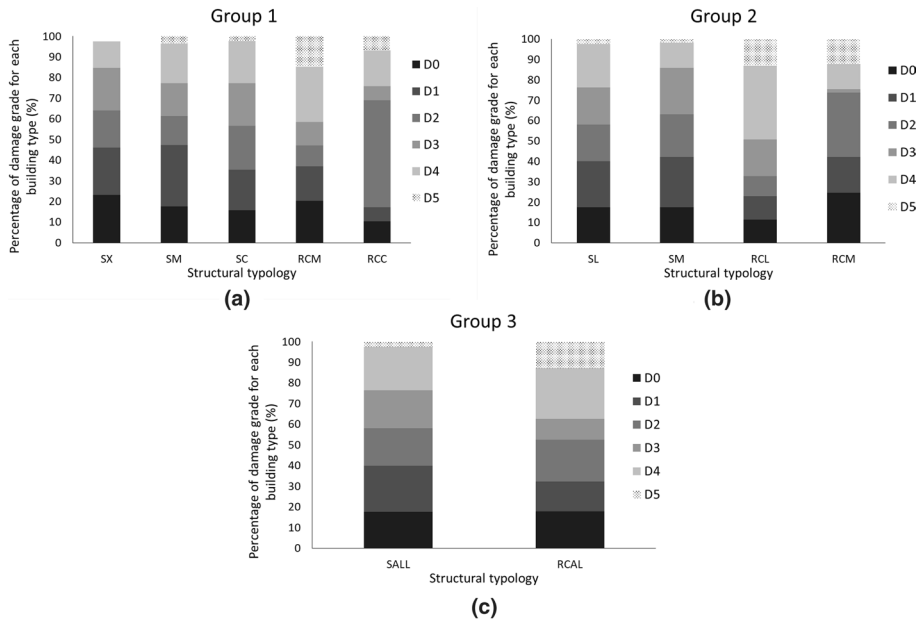


Fig. 2 Cumulative percentage of steel and RC buildings as a function of damage grade: **a** group 1 (different seismic resistant systems), **b** group 2 (different height), and **c** group 3 (total data for steel and RC structures)

4 Damage probability matrix and vulnerability index

According to the RISK-UE LM1 method (Milutinovic and Trendafiloski 2003), the damage probability matrices (DPMs) are required to determine the mean damage grade (μ_D), vulnerability index (V_I) and, consequently, the proposal of the empirical fragility curves. The DPM concept was developed by Withman et al. (1973) and is defined through a matrix, where each constitutive element represents the probability of a building to suffer a particular damage level under a specific ground motion. In this study, based on the structural damage survey of engineered steel and RC buildings affected by the devastating earthquake in Sarpol-e-zahab area, DPMs are developed in terms of PGA and EMS-98 intensity (Grünthal 1998). Figure 3 shows the damage grade variation with PGA of each building group by bar line graphs. Besides, PGA is converted to intensity using Eq. (1) and Table 3 presents the DPMs in terms of intensity for all three groups of steel and RC buildings.

DPM for each building with a specific seismic resistant system is formed of different damage levels at a specific PGA or its corresponding intensity. DPM provides a continuous parameter, which is defined as the mean damage ratio (μ_D). According to the RISK-UE LM1 method (Milutinovic and Trendafiloski 2003), the mean damage ratio can be calculated by Eq. (2):

$$\mu_D = \sum_{k=0}^5 p_k k \dots 0 < \mu_D < 5 \tag{2}$$

where p_k is the probability of experiencing a damage grade, equal to k , in a set of buildings.

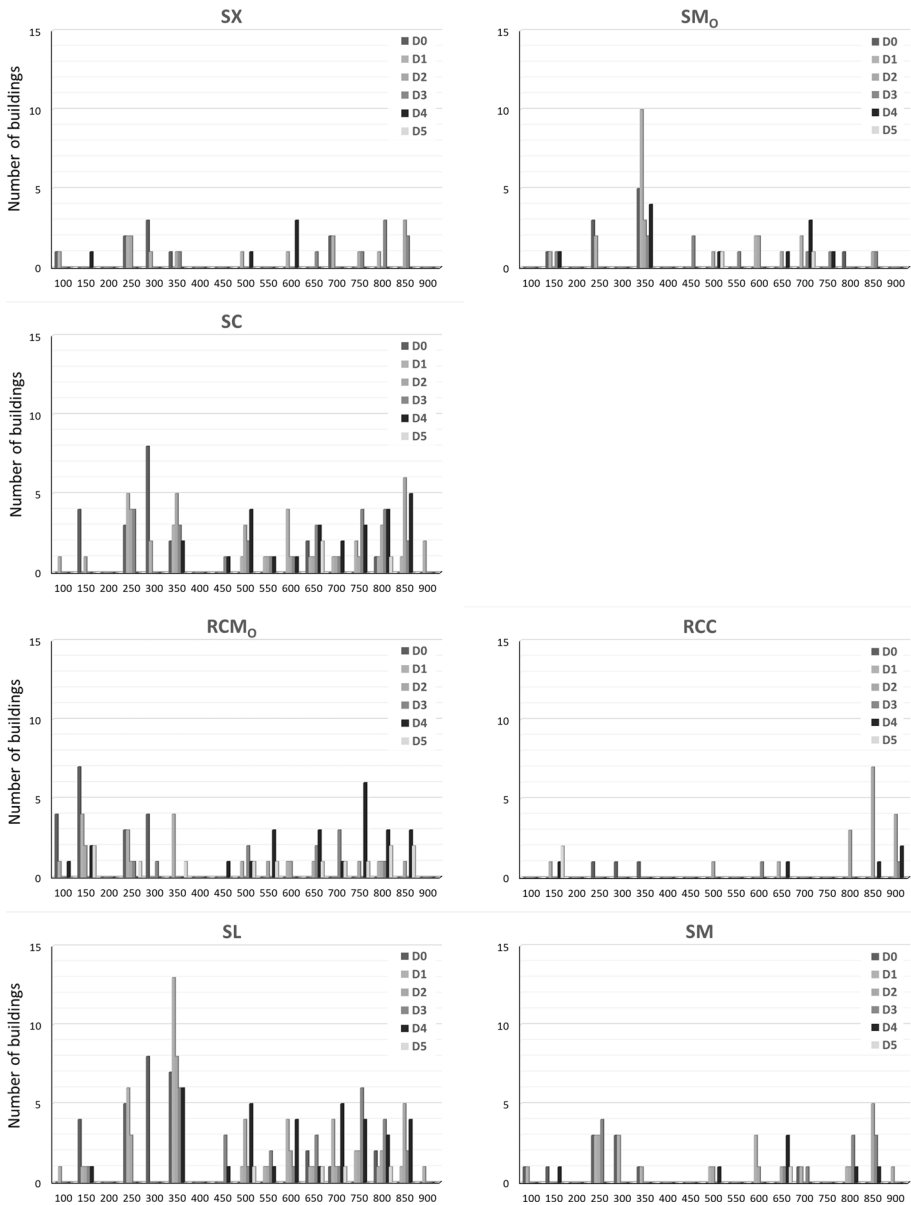


Fig. 3 Damage grade variation with PGA of each building type described in Table 2

The best-fitted power curve formulation between μ_D and PGA for each building type is used to derive the fragility curve in the next step. Furthermore, the mean value offers the seismic vulnerability index (V_p). The seismic vulnerability index is a score that quantifies the general seismic behavior of the buildings. According to Milutinovic and Trendafiloski (2003), the seismic vulnerability index ranges between 0 (for less vulnerable buildings) and 1 (for the most vulnerable buildings). The RISK-UE (LM1)

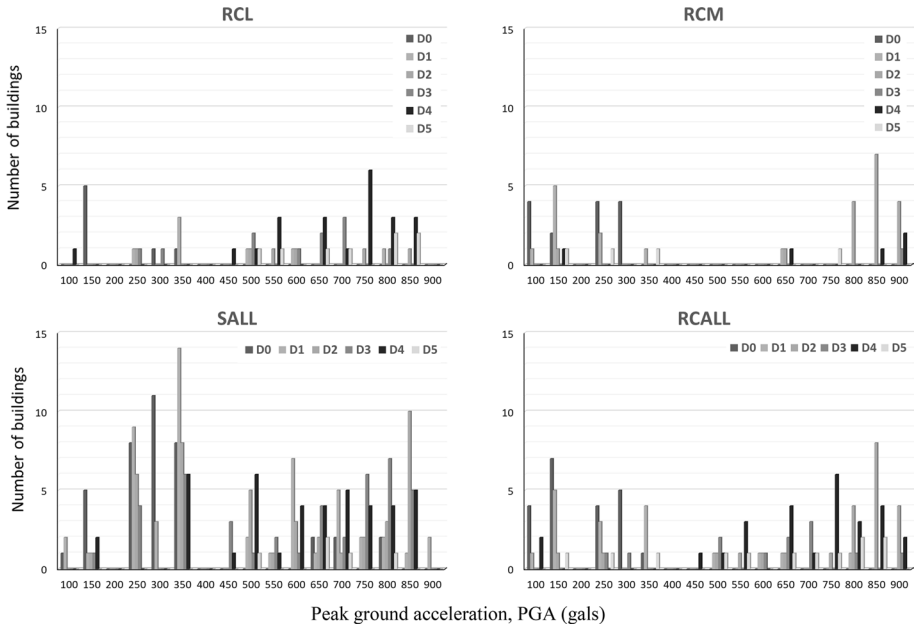


Fig. 3 (continued)

method (Milutinovic and Trendafiloski 2003) defines a mean semi-empirical seismic vulnerability function, that correlates the mean damage grade μ_D with both the EMS-98 intensity (Grünthal 1998) (I) and the seismic vulnerability index V_I , as reported in Eq. (3);

$$\mu_D = 2.5 \left[1 + \tanh \left(\frac{I + 6.25V_I - 13.1}{2.3} \right) \right] \tag{3}$$

Table 4 shows the seismic vulnerability index (V_I) for any structural seismic resistant systems investigated in this study. It shows that the seismic vulnerability of steel structures ($V_I=0.52-0.54$) is generally less than RC structures one ($V_I=0.6$). Poor monitoring of the implementation of seismic regulations during construction, as well as scarce or lack of geotechnical investigation and seismic microzonation, are the main reasons for these high seismic vulnerability index values for engineered structures, despite the compulsion to implement seismic regulations since 30 years ago. Meanwhile, the higher seismic vulnerability of RC buildings compared to steel buildings may be due to the use of the low strength concrete produced by the local concrete factories compared to the high-quality standard steel profiles.

An empirical assessment of the damage on the existing structures after a large earthquake can provide values of the vulnerability index due to these construction issues. These indices are useful for rapid damage assessment after an event or for the prediction of seismic vulnerability and risk for similar buildings.

Table 3 Damage probability matrix for each building type described in Table 2 relating intensities to damage grades

Group	SX	SM _O												
		D0	D1	D2	D3	D4	D5	D0	D1	D2	D3	D4	D5	
1	VII	1	1			1		1	1		1	1		
	VIII	2	2	2				3	2					
	IX	4	1	1	1			5	10	3	2	4		
	X		2			4			2	3	3	1	1	
	XI	2	3	4	7			1	2	2	3	5	1	
		SC	RCM _O											
		D0	D1	D2	D3	D4	D5	D0	D1	D2	D3	D4	D5	
	VII	4	1	1				11	5	2		3	2	
	VIII	3	5	4	4			3	3	1	1		1	
	IX	10	5	5	3	2		4	4		1		1	
	X		6	5	5	7			2	2	2	5	2	
	XI	3	8	12	14	17	3		1	4	6	16	7	
		RCC												
		D0	D1	D2	D3	D4	D5							
	VII		1			1	2							
	VIII	1												
IX	2													
X			1	1										
XI		1	14	1	4									
2		SL	SM											
		D0	D1	D2	D3	D4	D5	D0	D1	D2	D3	D4	D5	
	VII	4	2	1	1	1		2	1			1		
	VIII	5	6	3				3	3	3	4			
	IX	15	13	8	6	6		4	3	1				
	X		6	7	7	11	1		4	1	1	1		
	XI	5	10	11	16	17	3	1	3	7	8	5	1	
		RCL	RCM											
		D0	D1	D2	D3	D4	D5	D0	D1	D2	D3	D4	D5	
	VII	5				1		6	6	2		3	4	
	VIII		1	1	1			4	2				1	
	IX	2	3		1			4	1				1	
	X		2	3	3	5	2	0						
	XI		1	2	6	16	6	0	1	16	1	4	1	
	3		SAll	RCAll										
			D0	D1	D2	D3	D4	D5	D0	D1	D2	D3	D4	D5
VII		4	2	1	1	1		11	6	2		4	4	
VIII		5	6	3				4	3	1	1		1	
IX		15	13	8	6	6		6	4		1		1	
X			6	7	7	11	1		2	3	3	5	2	
XI		5	10	11	16	17	3		2	18	7	20	7	

Table 4 Seismic vulnerability index (V_I) for different typologies

Group	Type	Structural description	Proposed V_I
1	SX	Steel braced frame	0.52
	SM _O	Steel moment frame	0.54
	SC	Steel combination of moment and braced frame	0.52
	RCM _O	reinforced concrete moment frame	0.60
	RCC ^a	reinforced concrete combination of moment and RC shear wall	0.60
2	SL	Low-rise steel	0.54
	SM	High-rise steel	0.52
	RCL	Low-rise reinforced concrete	0.58
	RCM	High-rise reinforced concrete	0.55
3	SAll	Steel	0.54
	RCAI	Reinforced concrete	0.58

^aFor these building types, the number of inventoried buildings is less than 30 and the proposed values may be considered only as provisional indications

5 Empirical fragility curves

Fragility curves give the probability of reaching or exceeding specific damage grades under each level of ground motion parameters (GMP), as reported in the following equation:

$$P(DG \geq dg|GMP) \quad (4)$$

The most extensively used GMPs in the past for proposing the fragility curves were the various kinds of intensities. These parameters do not need any instrumental measuring and are directly determined from the structural damage caused by earthquakes. The RISK-UE (LM1) method (Milutinovic and Trendafiloski 2003) also used EMS-98 intensity (Grünthal 1998). Horizontal Peak Ground Displacement (PGD), horizontal Peak Ground Velocity (PGV) and Horizontal Peak Ground Acceleration (PGA) may be other single-point amplitude parameters. These parameters need instruments and a micro-shakemap from site response analysis. Since the accuracy of PGD and PGV are extensively dependent on filtering and baseline corrections, PGA is more appropriate for structural fragility studies. Meanwhile, considering natural frequency compatibility between the structures and the parameter frequency content, PGV can be more suitable for high-rise structures than low to mid-rise ones. The other parameter introduced for fragility studies in the literature is the elastic spectra (Spence et al. 1992; Singhal and Kiremidjian 1996; Rossetto 2004), which provide conservative results. In this study, low to mid-rise structures were concerned and, hence, the fragility curves are derived for PGAs (from 50 to 900 gals), as well as for EMS-98 intensities (Grünthal 1998) (from V to XI).

There are several main functional forms and regression techniques to propose fragility curves based on the lognormal cumulative distribution function, the exponential model function, and the beta distribution function. In this study, according to the RISK-UE (LM1) method (Milutinovic and Trendafiloski 2003), the beta distribution of mean damage grade is used. Equations (5)–(8) presented by Milutinovic and Trendafiloski (2003) show adequate formulations for deriving the damage distribution using the beta distribution.

$$p_{\beta}(x) = \frac{\Gamma(t)}{\Gamma(r)\Gamma(t-r)} \frac{(x-a)^{r-1}(b-x)^{t-r-1}}{(b-a)^{t-1}} a \leq x < b \tag{5}$$

$$P_{\beta}(x) = \int_a^x p_{\beta}(\varepsilon) d\varepsilon \tag{6}$$

where, $a = 0; b = 6; t = 8; r = t(0.007\mu_D^3 - 0.052\mu_D^2 + 0.287\mu_D)$, being $a, b, t,$ and r the parameters of the distribution and x is the continuous variable, which varies between a and b .

The discrete beta density probability function is calculated from the probabilities associated with damage grades k and $k + 1$ ($k = 0, 1, 2, 3, 4, 5$), as shown in Eq. (7):

$$p_k = P_{\beta}(k + 1) - P_{\beta}(k) \tag{7}$$

The fragility curve defining the probability of reaching or exceeding certain damage grades is obtained directly from the cumulative probability beta distribution, as shown in Eq. (8):

$$P(D \geq D_k) = 1 - P_{\beta}(k) \tag{8}$$

Based on the described RISK-UE (LM1) methodology, two sets of fragility curves, one as a function of PGA (Fig. 4) and the other as a function of EMS-98 intensity (Fig. 5), are derived from the Sarpol-e-zahab damage survey for all three groups of steel and RC structures. The fragility curves are presented for all introduced structural systems described in Table 2, except for RC structure with a combination of moment resisting frame and RC shear wall, whose database was limited to less than 30 cases.

6 Comparison with literature’s fragility curves

The proposed fragility curves are compared with those derived from previous researches. Figures 6, 7 and 8 show the comparison between fragility curves of this study for Steel and RC buildings and the existing fragility curves in terms of PGA found in the literature. However, since the considered fragility curves are based on four-level damages of HAZUS (1999), founded on collected data and beta distribution, four-level fragility curves are regenerated for better comparisons. To this aim, based on Rossetto and Elnashai’s (2003) damage scale correlation, slight damage grade for HAZUS (1999) is equal to D1 and D2 damage grades for EMS-98 intensity (Grünthal 1998).

Firstly, the expert judgment-based fragility curves proposed by Fallah Tafti et al. (2020) for the common types of buildings in Iran are discussed. For low-rise and mid-rise high-code steel structures see Fig. 6a, b and for RC ones see Fig. 6c, d. Generally, Fallah Tafti et al. (2020) fragility curves (gray lines) show a rather higher fragility at all damage grades for both steel and RC structures compared to those proposed herein (black lines). The only exception is for RC and steel low-rise structures, which experienced slight damages according to the Fallah Tafti et al. (2020) predictions. It seems that, at least in small cities of Iran, the low quality of both materials and construction control due to weak economy and insufficient experience of engineers and constructors have raised the fragility of low-rise RC structures. However, this issue was neglected by experts. Meanwhile, experts

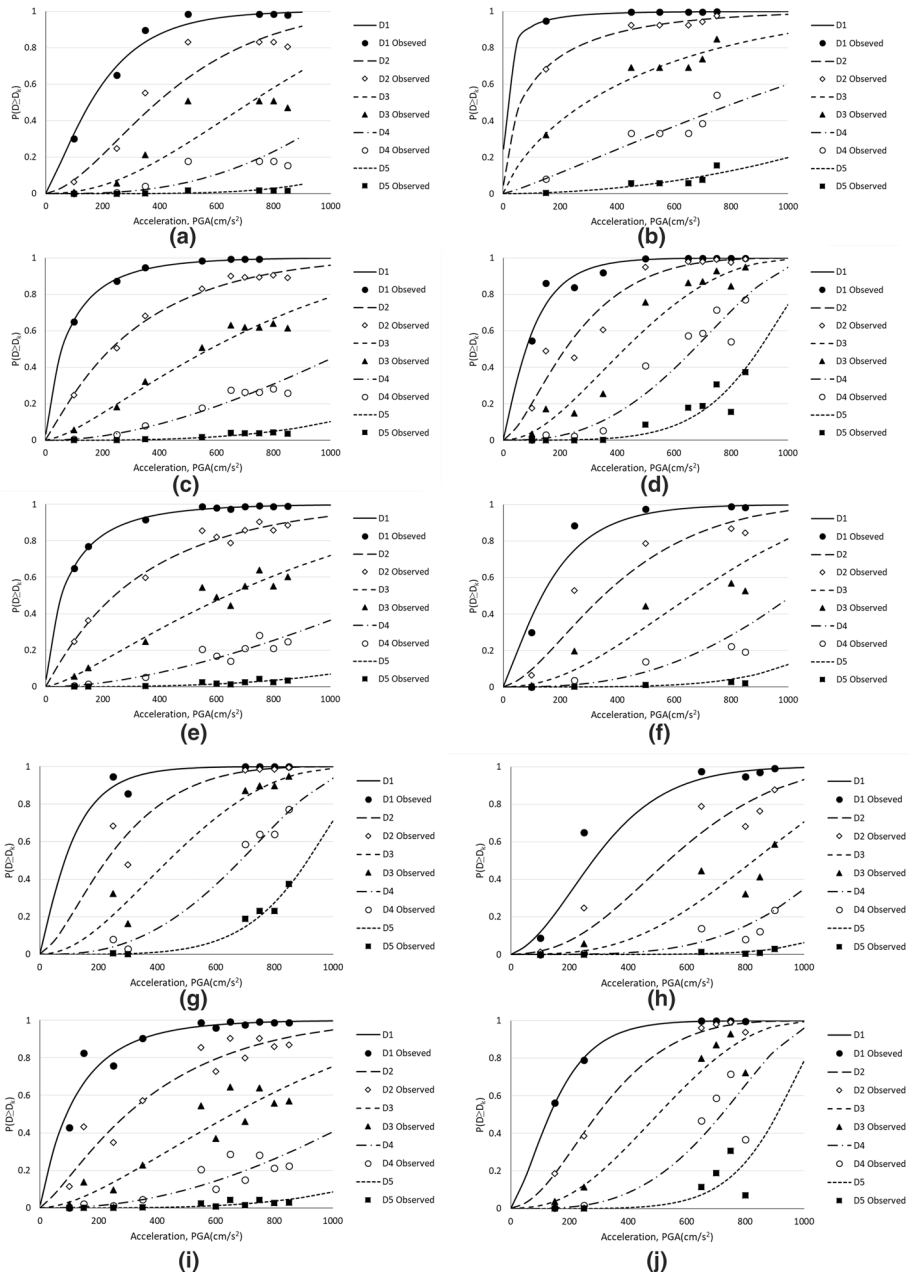


Fig. 4 Fragility curves (lines) fitting observed fragility data (dots) for the assumed building classes in terms of PGA **a** SX, **b** B_{M_0} , **c** SC, **d** RC_{M_0} , **e** SL, **f** SM, **g** RCL, **h** RCM, **i** SAIL, and **j** RCAL

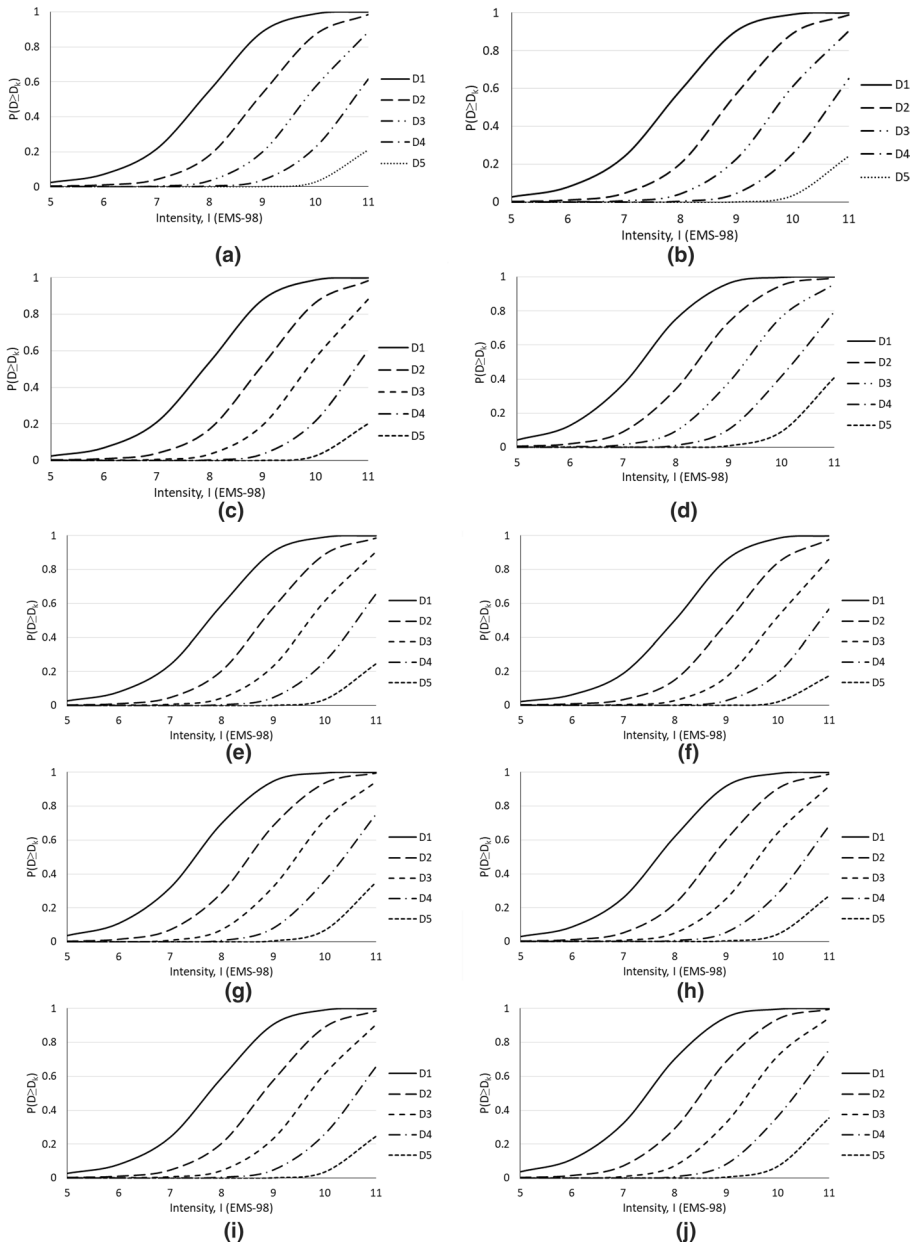


Fig. 5 Fragility curves in terms of Ems-98 intensity, **a** SX, **b** SM_0 , **c** SC, **d** RCM_0 , **e** SL, **f** SM, **g** RCL, **h** RCM, **i** SAll, and **j** RCall

expected more damage to medium-rise RC buildings. It is more likely expected that expert judgment-based fragility curves should not underestimate the empirical fragility curves.

Secondly, the empirical fragility curves proposed from DPMs by Lagomarsino and Giovinazzi (2006), and Del Gaudio et al. (2017) for low-rise and mid-rise RC buildings

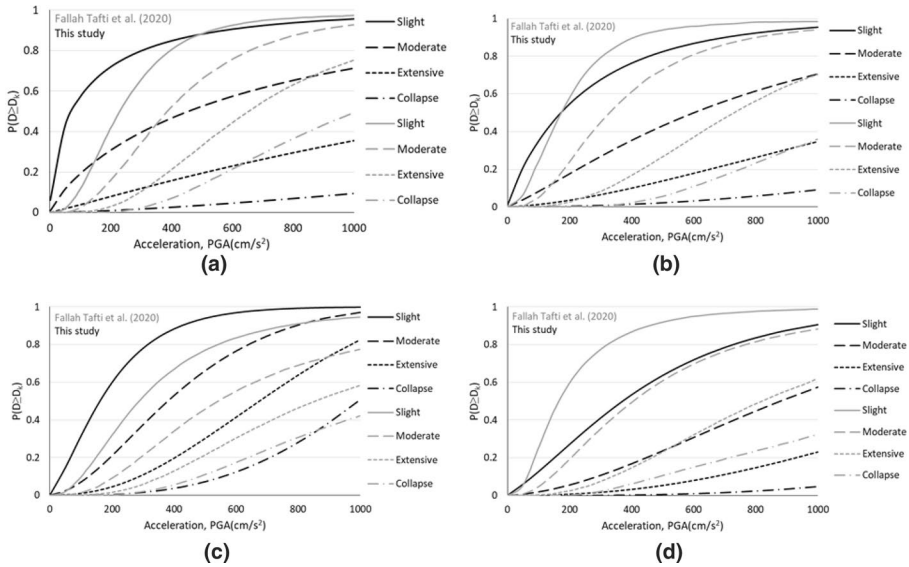


Fig. 6 Comparison between empirical fragility curves proposed herein (black lines) and by Fallah Tafti et al. (2020) (gray lines) in terms of PGA, **a** SL, **b** SM, **c** RCL, and **d** RCM

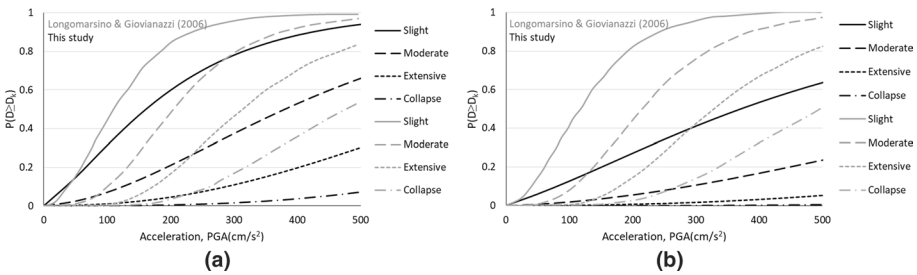


Fig. 7 Comparison between empirical fragility curves proposed herein (black lines) and by Longomarsino and Giovanazzi (2006) (gray lines) in terms of PGA, **a** RCL, and **b** RCM

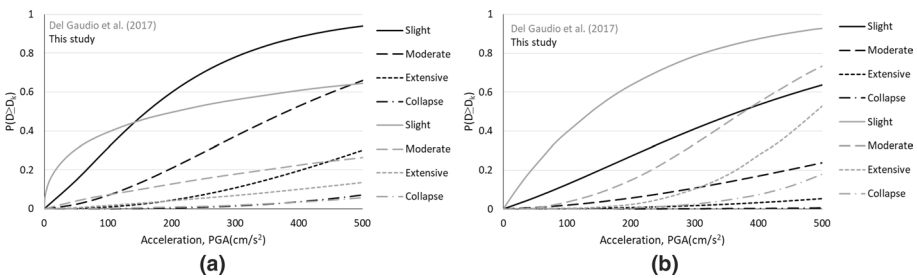


Fig. 8 Comparison between empirical fragility curves proposed herein (black lines) and by Del Gaudio et al. (2017) (gray lines) in terms of PGA, **a** RCL, and **b** RCM

are compared. The fragility curves provided by Lagomarsino and Giovinazzi (2006) for low-rise (Fig. 7a) and mid-rise (Fig. 7b) RC structures (gray lines), show a higher fragility at all damage grades compared to those proposed from the Sarpol-e-zahab earthquake (black lines). In mid-rise RC structures the fragility curves of Lagomarsino and Giovinazzi (2006) are significantly higher than the ones of this study. This shows that the fragility curves of Lagomarsino and Giovinazzi (2006) would evaluate the fragility of mid-rise RC structures of Iran even more conservatively. Instead, the empirical fragility curves proposed by Del Gaudio et al. (2017) for Italian low-rise RC structures (Fig. 8a) are more realistic than the ones of Lagomarsino and Giovinazzi (2006). These curves show less fragility for low-rise Italian RC structures than the ones in Iran. However, the mid-rise Iranian RC structures still show less fragility than Italian ones (Fig. 8b).

Finally, the proposed empirical fragility curves in terms of EMS-98 intensity (Grünthal 1998) for steel braced frame, steel moment frame and RC moment frame buildings are compared with the empirical fragility curves of the same type of buildings proposed by Omidvar et al. (2012) from damage data of 2003 Bam earthquake (M_w 6.6) in central Iran. They used the RISK-UE (LM1) method (Milutinovic and Trendafiloski 2003) and the beta distribution of mean damage grade. Figure 9 shows this comparison. It is noteworthy that the empirical fragility curves proposed by Omidvar et al. (2012) for engineered steel and RC structures, are based on limited data (number of investigated $SX=28$, $SMo=10$, and $RCMo=10$), and were the only empirical fragility curves for engineered steel and RC buildings in Iran. According to Fig. 9, a good agreement is observed between the fragility curves of this study and the fragility curves derived from the DPMs proposed by Omidvar et al. (2012) in terms of Intensity from the Bam earthquake at all damage grades.

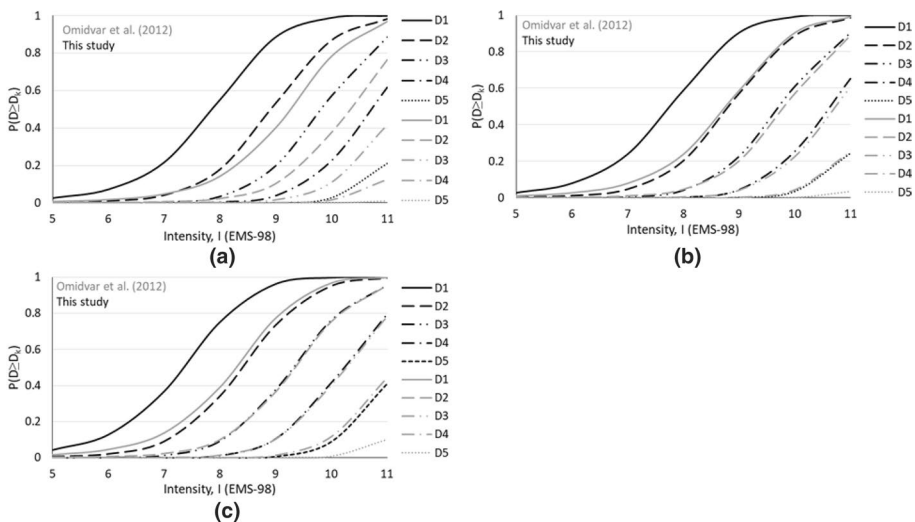


Fig. 9 Comparison between empirical fragility curves proposed herein (black lines) and by Omidvar et al. (2012) (gray lines) in terms of EMS-98 intensity, **a** SX , **b** SMo , and **c** $RCMo$

7 Conclusions

After the occurrence of M_w 7.3 2017 earthquake in Kermanshah province near the Iran-Iraq border, very heavy to destructive structural damage was observed in cities and villages in the west and northwest of Kermanshah province, especially in the city of Sarpol-e-zahab, which was located about 35 km far from the epicenter. Most of the buildings in these areas have been renovated, after the damage caused by the 1980 to 1988 war, with earthquake-resistant steel and RC frames. Damage observations from this earthquake provided damage data of the sufficient number of engineered steel and RC structures for the first time in the history of earthquakes in Iran. Accordingly, in this study, using the collected structural damage data after the event, empirical fragility curves were presented for various seismic resistant structural systems of steel and RC buildings for both low-rise and mid-rise heights. The questioned seismic-resistant systems were steel braced frames, steel and RC moment-resisting frames, the combination of steel moment-resisting frame and steel braced frame and the combination of RC moment-resisting frame and RC shear wall.

As a novel study of empirical fragility curves in terms of PGA for engineered structures in Iran, the comprehensive microzonation studies, accompanied by the seismic site response analyses in Sarpol-e-zahab city, along with data recorded by ISMN's stations, and the shakemap for Kermanshah province from the literature, have provided the PGA experienced by each investigated structure during M^w 7.3 earthquake event. This has reduced the uncertainty on the expected strong-motion beneath each investigated building in the empirical fragility curves. Meanwhile, as a remaining limitation of the empirical fragility curves of this study, they are based on a single earthquake and it shows the importance of similar studies that should be performed after forthcoming catastrophic earthquakes in Iran. Besides, using the relationships between PGA and intensity, the empirical fragility curves in terms of intensity were also proposed.

Accordingly, the proposed empirical fragility curves were compared with the literature fragility curves for similar structures in Iran and Italy, both in terms of PGA and intensity. The results showed that the Iranian expert judgment-based fragility curves for low-rise high-code RC structures, estimated less damage level than the realistic empirical fragility curves of this study. Contrary, in other structural systems and heights, expert judgment-based fragility curves were conservative. The empirical fragility curves for Italian low-rise and mid-rise RC structures provided conservative damages than the empirical fragility curves of this study. Finally, the new empirical fragility curves presented in terms of intensity were in good agreement with the only empirical fragility curves of steel and RC buildings in Iran, which were calculated from the limited available damage data from the Bam earthquake.

These new empirical fragility curves can be useful in the rapid assessment of seismic damage to Iranian cities, as well as for predicting seismic risk and vulnerability in various future scenarios.

Acknowledgements The Authors wishes to forward thanks to anonymous reviewers of the manuscript for the time and effort that dedicated to the review, which improved the quality of the paper.

Author's contributions Term: Mahnoosh Biglari Conceptualization: Mahnoosh Biglari, Antonio Formisano Methodology: Mahnoosh Biglari, Antonio Formisano Validation: Mahnoosh Biglari, Antonio Formisano, Behrokh Hosseini Hashemi Formal analysis: Mahnoosh Biglari Writing—original draft preparation: Mahnoosh Biglari Writing—review and editing: Mahnoosh Biglari, Antonio Formisano, Behrokh Hosseini Hashemi Resources: Mahnoosh Biglari, Behrokh Hosseini Hashemi Visualization: Mahnoosh Biglari, Antonio Formisano, Behrokh Hosseini Hashemi.

Funding No Funding.

Availability of data and material Not Applicable.

Declarations

Conflict of interest No Conflicts of interest.

Code availability Not Applicable.

References

- Ashayeri I, Sadr A, Biglari M, Haghshenas E (2020) Comprehensive ambient noise analyses for seismic microzonation of sarpol-e-zahab after the Mw 7.3 2017 Iran earthquake. *Eng Geol.* <https://doi.org/10.1016/j.enggeo.2020.105636>
- Ashayeri I, Memari A, Haghshenas E (2021) Seismic microzonation of Sarpol-e-zahab after Mw 7.3 2017 Iran earthquake: 1D-equivalent linear approach. *Bull Earthq Eng* 19:605–622. <https://doi.org/10.1007/s10518-020-00999-6>
- Azzaro R, Barbano MS, Camassi R, D'Amico S, Mostaccio A, Piangiamore G, Scarfi L (2004) The earthquake of 6 September 2002 and the seismic history of Palermo (Northern Sicily, Italy): Implications for the seismic hazard assessment of the city. *J Seismol* 8:525–543. <https://doi.org/10.1007/s10950-004-8930-2>
- Biglari M, Formisano A (2020) Damage probability matrices and empirical fragility curves from damage data on masonry buildings after Sarpol-e-zahab and bam earthquakes of Iran. *Front Built Environ.* <https://doi.org/10.3389/fbuil.2020.00002>
- Del Gaudio C, De Martino G, Di Ludovico M, Manfredi G, Prota A, Ricci P, Verderame G (2017) Empirical fragility curves from damage data on RC buildings after the 2009 L'Aquila earthquake. *Bull Earthq Eng* 15:1425–1450. <https://doi.org/10.1007/s10518-016-0026-1>
- Fallah Tafti M, Amini Hosseini K, Mansouri B (2020) Generation of new fragility curves for common types of buildings in Iran. *Bull Earthq Eng* 18:3079–3099. <https://doi.org/10.1007/s10518-020-00811-5>
- Firuzi E, Ansari A, Rashidabadi M, Amini-Hosseini K (2018) Developing ground motion shaking map for sarpol-e zahab, Iran (2017) earthquake. *J Seismol Earthq Eng* 20:45–55
- Gomez-Capera AA, D'Amico M, Lanzano G, Locati M, Santulin M (2020) Relationships between ground motion parameters and macroseismic intensity for Italy. *Bull Earthq Eng* 18:5143–5164. <https://doi.org/10.1007/s10518-020-00905-0>
- Grünthal G. (ed.) (1998) Cahiers du Centre Européen de Géodynamique et de Séismologie. Vol 15, European Macroseismic Scale. Luxembourg: European Center for Geodynamics and Seismology
- HAZUS (1999) Federal Emergency Management Agency. HAZUS user and technical manuals. Federal Emergency Management Agency Report, Washington D.C., Vol. 7, 1999.
- Kalantari A, Hashemi BH, Sarvghad Moghadam A, Mansouri B, Farshchi HR (2019) Buildings damage data gathering after 2017 Sarpol-e-zahab earthquake. In: 8th International conference on earthquake engineering and seismology, Tehran:11–13.
- Lagomarsino G, Giovinazzi S (2006) Macroseismic and mechanical models for the vulnerability and damage assessment of current buildings. *Bull Earthq Eng* 4:415–443. <https://doi.org/10.1007/s10518-006-9024-z>
- Milutinovic ZV, Trendafiloski GS (2003) RISK-UE. An advanced approach to earthquake risk scenarios with applications to different european towns, WP4: vulnerability of current buildings, Contract: EVK4-CT-2000-00014
- Omidvar B, Gatmiri B, Derakhshan S (2012) Experimental vulnerability curves for the residential buildings of Iran. *Nat Hazards* 60:345–365. <https://doi.org/10.1007/s11069-011-0019-y>
- RISK-UE (2004) The European Risk-UE project: an advanced approach to earthquake risk scenarios. (2001–2004), <http://www.risk-ue.net>
- Rossetto T (2004) Vulnerability curves for the seismic assessment of reinforced concrete structure populations. PhD Thesis, Imperial College, London, UK.
- Rossetto T, Elnashai A (2003) Derivation of vulnerability functions for European-type RC structures based on observational data. *Eng Struct* 25(10):1241–1263. [https://doi.org/10.1016/S0141-0296\(03\)00060-9](https://doi.org/10.1016/S0141-0296(03)00060-9)

- Sieberg A (1930) The earthquake geology (Geologie der Erdbeben). Handbuch der Geophysik 2(4):550–555 ((in German))
- Singhal A, Kiremidjian AS (1996) Method for probabilistic evaluation of seismic structural damage. J Struct Eng ASCE 122:1459–1467. [https://doi.org/10.1061/\(ASCE\)0733-9445\(1996\)122:12\(1459\)](https://doi.org/10.1061/(ASCE)0733-9445(1996)122:12(1459))
- Spence RJS, Coburn AW, Pomonis A (1992) Correlation of ground motion with building damage: the definition of a new damage-based seismic intensity scale. In: Proceedings of 10th world conference on earthquake engineering, Balkema, Rotterdam.
- Tatar M, Ghaemmaghamian MR, Yaminifard F, Hesamiazar K, Ansari A, Firouzi E (2018) Seismological Aspects, Reconnaissance of 12th Nov. 2017 Sarpol-e-zahab, Kermanshah Province Earthquake. 5th ed. Vol. 1, Tehran: IIEES (In Persian).
- Whitman RV, Reed JW, Hong ST (1973) Earthquake damage probability matrices. In Proceedings of the fifth world conference on earthquake engineering (Rome):2531–2540.

Publisher's Note Springer Nature remains neutral with regard to jurisdictional claims in published maps and institutional affiliations.

Authors and Affiliations

Mahnoosh Biglari¹  · Antonio Formisano²  · Behrokh Hosseini Hashemi³ 

Antonio Formisano
antoform@unina.it

Behrokh Hosseini Hashemi
behrokh@iiees.ac.ir

- ¹ Department of Civil Engineering, School of Engineering, Razi University, Member of IIEEA, P.O.Box: 67149-67346, Kermanshah, Iran
- ² Department of Structures for Engineering and Architecture, School of Polytechnic and Basic Sciences, University of Naples Federico II, Naples, Italy
- ³ Department of Structures, International Institute of Earthquake Engineering and Seismology (IIEES), Member of IIEEA., Tehran, Iran